12-2020

Parton Distribution Functions from Ioffe time Pseudodistributions from Lattice Calculations: Approaching the Physical Point

Bálint Joó

Joseph Karpie

Kostas Orginos

Anatoly V. Radyushkin
Old Dominion University, aradyush@odu.edu

David G. Richards

See next page for additional authors

Original Publication Citation

Joó, B., Karpie, J., Orginos, K., Radyushkin, A. V., Richards, D. G., & Zafeiropoulos, S. (2020). Parton distribution functions from Ioffe time pseudodistributions from lattice calculations: Approaching the physical point. *Physical Review Letters,* 125, 1-7, Article 232003. https://doi.org/10.1103/PhysRevLett.125.232003

Parton Distribution Functions from Ioffe Time Pseudodistributions from Lattice Calculations: Approaching the Physical Point

Bálint Joó,[1,2] Joseph Karpie,[3] Kostas Orginos,[2,4] Anatoly V. Radyushkin,[2,5] David G. Richards,[2] and Savvas Zafeiropoulos[6]

[1]Oak Ridge Leadership Facility, Oak Ridge National Laboratory, One Bethel Valley Road, Oak Ridge, Tennessee 37831, USA
[2]Thomas Jefferson National Accelerator Facility, Newport News, Virginia 23606, USA
[3]Physics Department, Columbia University, New York City, New York 10027, USA
[4]Physics Department, College of William and Mary, Williamsburg, Virginia 23187, USA
[5]Physics Department, Old Dominion University, Norfolk, Virginia 23529, USA
[6]Aix Marseille Univ, Université de Toulon, CNRS, CPT, Marseille, France

(Received 9 April 2020; revised 27 July 2020; accepted 9 September 2020; published 1 December 2020)

We present results for the unpolarized parton distribution function of the nucleon computed in lattice QCD at the physical pion mass. This is the first study of its kind employing the method of Ioffe time pseudodistributions. Beyond the reconstruction of the Bjorken-x dependence, we also extract the lowest moments of the distribution function using the small Ioffe time expansion of the Ioffe time pseudodistribution. We compare our findings with the pertinent phenomenological determinations.

DOI: 10.1103/PhysRevLett.125.232003

Introduction.—The determination and understanding of the internal quark and gluon structure of the proton is a crucial aspect of the precision phenomenology program of the current and future hadron collider experiments, especially the Large Hadron Collider (LHC) and the upcoming Electron-Ion Collider. The framework of collinear factorization quantifies the hadronic structure in terms of parton distribution functions (PDFs) which encapsulate the pertinent information regarding the momentum distributions of quarks and gluons within the nucleon. Until very recently, the intrinsic nonperturbative nature of the PDFs prohibited an *ab initio* computation, and the conventional approach is to employ a variety of experimental data together with advanced fitting methodologies in order to extract the PDFs via global fits. The studies of PDFs are of paramount importance precisely due to the fact that their uncertainties play a crucial role in many LHC applications. They affect the measurement of precision standard model (SM) parameters, such as the W mass, the strong coupling constant, and the determination of the couplings of the Higgs boson, where discrepancies from the stringently fixed SM predictions would serve as indisputable evidence of beyond the standard model physics [1].

The possibility of determining the PDFs with first principle lattice calculations is the object of a long endeavor which recently led to a culmination of results. The primary difficulty impeding a first principle implementation is associated with the fact that the matrix elements defining the PDFs involve light-cone separated fields. In his seminal article that stimulated recent efforts, Ji [2] proposed to compute matrix elements of fields separated by a purely spacelike distance $z = z_3$ that define the so-called quasi-PDF, the distribution in the longitudinal momentum p_3. In the large p_3 limit, they can be factorized into the light-cone PDF, $f(x, \mu^2)$. Subsequently, many articles studying quasi-PDFs, as well as the pion quasidistribution amplitude (DA), appeared in the literature [3–24].

Alternative approaches based on the analysis of equal-time current correlators [25–28] also aim to study the PDFs or DAs in lattice QCD. Good lattice cross sections (LCSs), as described in Ref. [29], represent a general framework, where one computes matrix elements that can be factorized into PDFs at short distances. References [30–34] fall into these categories. For comprehensive reviews on the topic, we refer the reader to Refs. [35–38].

Ioffe time pseudodistributions.—Another position-space formulation was proposed in Ref. [39]. In this approach, the basic object is the Ioffe time pseudodistribution function (pseudo-ITD) $\mathcal{M}(\nu, z^2)$. The Lorentz invariant $\nu = pz$ is known as the Ioffe time [40,41]. The pseudo-ITD is the invariant amplitude for a matrix element with spacelike separated quark fields.

In renormalizable theories, the pseudo-ITD exhibits a logarithmic singularity at small values of z^2. These short-distance singularities can be factorized into the PDF and a perturbatively calculable coefficient function. The pseudo-ITD can also be considered a LCS. A series of works implemented this formalism and studied its efficiency

[42–47]. For the sake of completeness, the main points of our formalism are summarized below, but we refer the reader to Refs. [46,48] for detailed discussions.

The nonlocal matrix element,

$$M^{\alpha}(p,z) = \langle p|\bar{\psi}(z)\gamma^{\alpha}U(z;0)\psi(0)|p\rangle, \tag{1}$$

with U being a straight Wilson line, $p=[p^+,(m^2/2p^+),0_T]$, $z=(0,z_-,0_T)$ and $\gamma^a=\gamma^+$ in light-cone coordinates, defines the modified minimal subtraction ($\overline{\rm MS}$) ITD (introduced in Ref. [41]), given the fact that a regularization is made for the $z^2=0$ singularity. For $z^2\neq 0$, this matrix element has the following Lorentz decomposition:

$$M^{\alpha}(z,p) = 2p^{\alpha}\mathcal{M}(\nu,z^2) + 2z^{\alpha}\mathcal{N}(\nu,z^2). \tag{2}$$

The pseudo-ITD $\mathcal{M}(\nu,z^2)$ contains the leading twist contribution, while $\mathcal{N}$ is a higher-twist term. In the kinematics $p=(E,0,0,p_3)$, $z=(0,0,0,z_3)$, the choice $\alpha=0$ isolates $\mathcal{M}$. Nonetheless, it still contains higher-twist contaminations $O(z^2\Lambda^2_{\rm QCD})$. In the limit of small z^2, where higher-twist terms are suppressed, $\mathcal{M}$ is factorizable into the ITD (or, equivalently, the PDF) and a perturbative coefficient function, provided that one removes Wilson line–related UV divergences that appear at finite z^2. These UV divergences are eliminated if one considers the reduced pseudo-ITD [39,42] given by the ratio

$$\mathfrak{M}(\nu,z^2) = \frac{\mathcal{M}(\nu,z^2)}{\mathcal{M}(0,z^2)}. \tag{3}$$

It contains the same singularities in the $z^2=0$ limit as $\mathcal{M}$ and can be related to the $\overline{\rm MS}$ light-cone ITD, $Q(\nu,\mu^2)$, by the next-to-leading-order (NLO) matching relation [49–51]

$$\mathfrak{M}(\nu,z^2) = Q(\nu,\mu^2) - \frac{\alpha_s C_F}{2\pi}\int_0^1 du Q(u\nu,\mu^2) \times\left[\ln\left(z^2\mu^2\frac{e^{2\gamma_E+1}}{4}\right)B(u)+L(u)\right], \tag{4}$$

where $B(u)=[1+u^2/1-u]_+$ is the Altarelli-Parisi kernel [52], and

$$L(u) = \left[4\frac{\ln(1-u)}{1-u} - 2(1-u)\right]_+. \tag{5}$$

Extracting the matrix element.—The numerical computation of our matrix elements relies on Gaussian smearing [53] and momentum smearing [54] for constructing the nucleon interpolating field, as well as the summation method for better control of the excited-state contamination. The latter is intimately related to the Feynman-Hellmann (FH) theorem [55] and has been widely used in lattice calculations of PDFs [18,20,21,42,43,46,47].

The matrix element is determined from a ratio of correlation functions

$$R(t) = \frac{\sum_{\tau} C_3(t,\tau)}{C_2(t)}, \tag{6}$$

where $C_{2,3}$ are standard two and three point correlation functions, t is the Euclidean separation between the source and sink interpolating fields, and the operator insertion time τ is summed over the entire temporal range. The effective matrix element $M^{\rm eff}$ is then constructed as

$$M^{\rm eff}(t) = R(t+1) - R(t). \tag{7}$$

The leading excited-state effects can be parametrized by

$$M^{\rm eff}(t) = M(1 + Ae^{-\Delta t} + Bte^{-\Delta t}), \tag{8}$$

with Δ being the energy gap between the ground state and the lowest excited state.

The summation method has a clear advantage over the typical ratio method. The excited-state contamination scales as $\exp(-\Delta t)$ instead of $\exp(-\Delta t/2)$, which allows for smaller t to be used to control excited-state effects. Since correlation functions' errors grow exponentially, the summation method requires significantly fewer measurements to obtain a desirable statistical precision for data with controlled excited states. This feature is important for calculations at large momenta, where energy gaps can be small and the error decays much faster than for low momenta.

Lattice QCD calculation.—In this Letter, three ensembles of configurations with decreasing values of the pion mass have been employed. In Table I, we list all the parameters of our analysis. The pion masses of this Letter are 172, 278, and 358 MeV. These ensembles allow for a controlled extrapolation to the precise physical pion mass, which constitutes an important limit to be taken in order to

TABLE I. Parameters for the lattices generated by the JLab/W&M Collaboration using $2+1$ flavors of stout-smeared clover Wilson fermions and a tree-level tadpole-improved Symanzik gauge action. More details about these ensembles can be found in Ref. [56].

ID	a (fm)	M_π (MeV)	β	$c_{\rm SW}$	am_l	am_s	$L^3\times T$	$N_{\rm cfg}$
$a094m360$	0.094(1)	358(3)	6.3	1.205 365 88	−0.2350	−0.2050	$32^3\times 64$	417
$a094m280$	0.094(1)	278(3)	6.3	1.205 365 88	−0.2390	−0.2050	$32^3\times 64$	500
$a091m170$	0.091(1)	172(6)	6.3	1.205 365 88	−0.2416	−0.2050	$64^3\times 128$	175

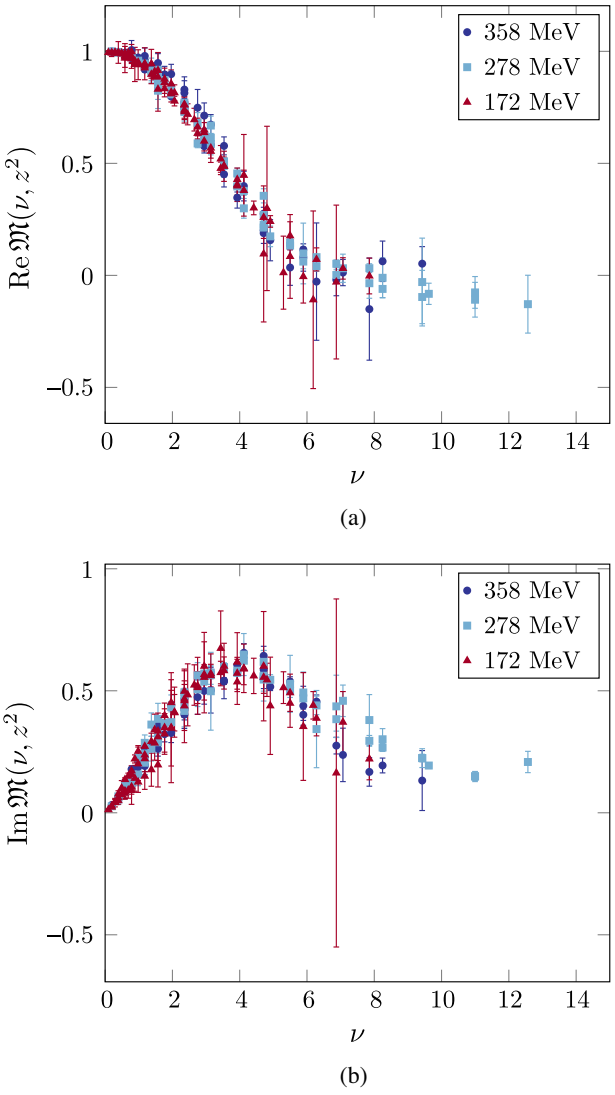

FIG. 1. The reduced pseudo-ITD calculated on ensembles with 358 MeV, 278 MeV, and 172 MeV pion masses. The upper and lower plots are the real and imaginary component respectively. There appear to be very small mass effects within this range of ν and z^2.

safely compare with the PDF determinations of global fits. Also, we can study the pion mass effects on the ITD for the first time. As was done in Ref. [46], correlation functions with several different smearings were simultaneously fit to determine the matrix element from Eq. (8). The matrix elements extracted from fitting correlation functions to Eq. (8) are shown in Fig. 1.

Moments of the PDF.—Following our suggestion in Ref. [44], we can use the reduced pseudo-ITD to compute the moments of the PDF. Valuable information for the PDF can be extracted from the data without dealing with the pitfalls of the inverse problem. The moments of the $\overline{\mathrm{MS}}$ PDF, $a_n(\mu^2)$, are related multiplicatively to those of the Fourier transform of the reduced pseudo-ITD,

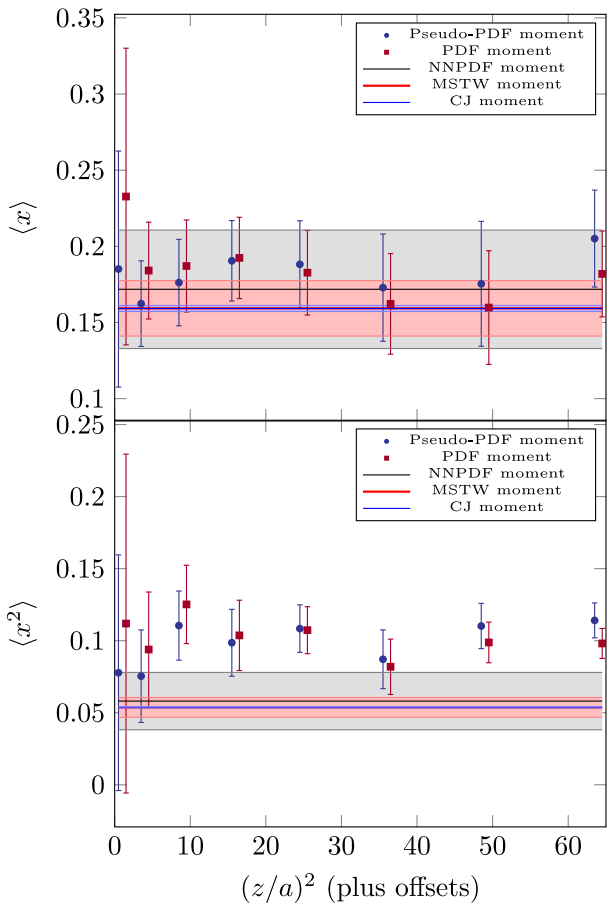

FIG. 2. The first two moments of the pseudo-PDF and the $\overline{\mathrm{MS}}$ light-cone PDF computed from the ensemble $a091m170$, compared to phenomenologically determined PDF moments from the NLO global fit CJ15nlo [57] and the next-to-next-to-leading (NNLO) global fits MSTW2008nnlo68cl_nf4 [58] and NNPDF31_nnlo_pch_as_0118_mc_164 [59], all evolved to 2 GeV.

$$b_n(z^2) = C_n(\mu^2 z^2) a_n(\mu^2) + \mathcal{O}(z^2 \Lambda^2_{\mathrm{QCD}}) \tag{9}$$

where C_n are the Mellin moments of the matching kernel $C(u, \mu^2 z^2)$ with respect to u. To NLO accuracy,

$$C_n(z^2\mu^2) = 1 - \frac{\alpha_s}{2\pi} C_F \left[\gamma_n \ln\left(z^2\mu^2 \frac{e^{2\gamma_E+1}}{4} \right) + l_n \right], \tag{10}$$

where

$$\gamma_n = \int_0^1 du B(u) u^n = \frac{1}{(n+1)(n+2)} - \frac{1}{2} - 2\sum_{k=2}^{n+1} \frac{1}{k} \tag{11}$$

are the moments of the Altarelli-Parisi kernel and

$$l_n = \int_0^1 du L(u) u^n = 2\left[\left(\sum_{k=1}^{n}\frac{1}{k}\right)^2 + \sum_{k=1}^{n}\frac{1}{k^2} + \frac{1}{2} - \frac{1}{(n+1)(n+2)}\right]. \quad (12)$$

The even and odd moments can be determined from the coefficients of polynomials which are fit to the real and imaginary components, respectively. The order of the polynomial is chosen to minimize the χ^2/DOF for each z^2 separately. As an example, the first and second moments calculated on the ensemble $a091m170$ are shown in Fig. 2. The z^2 dependence of the resulting PDF moments can be used to check for the size of higher-twist effects, which do not seem significant.

Matching to $\overline{\text{MS}}$.—As in Ref. [46], the reduced pseudo-ITD from each ensemble is matched to the light-cone $\overline{\text{MS}}$ ITD at a given scale μ by inverting Eq. (4). As a result, we obtain a set of z^2-independent curves for $Q(\nu, \mu^2)$ at $\mu = 2$ GeV [shown in Fig. 3(a)].

As seen in the moments, the matching procedure has a small $\mathcal{O}(\alpha_s/\pi) \sim 0.1$ effect on the distribution. The contributions from the convolution of B and L with the reduced pseudo-ITD appear with opposite signs. The convolution with L is slightly larger in magnitude, but by a factor which is approximately the same as the logarithmic coefficient of B. This feature may just be a coincidence at NLO, but it hints that higher-order corrections may also be small. An NNLO or nonperturbative matching is required to check the effects of the perturbative truncation on the matching.

Determination of the PDF.—The inversion of the Fourier transform defining the ITD, given a finite amount of data, constitutes an ill-posed problem which can be resolved only by including additional information. As was shown in Ref. [45], the direct inverse Fourier transform can lead to numerical artifacts, such as artificial oscillations in the resulting PDF. Many techniques have been proposed to accurately calculate PDFs from lattice data [21,28,45,60]. This issue also occurs in the determination of the PDF from experimental data.

As was done in Ref. [46], the approach which is used here (and is common among phenomenological determinations) is to include information in the form of a model-dependent PDF parametrization. The parametrization used here is

$$q_v(x) = \frac{1}{N} x^a (1-x)^b (1 + c\sqrt{x} + dx), \quad (13)$$

where N normalizes the PDF. The fits to this form, together with the bands representing the statistical errors on the fit, are shown in Fig. 3(b). In a future work, we will attempt to study the dependence on the choice of functional forms.

The results of these fits are largely consistent with each other. The heaviest pion mass PDF has a notably larger statistical error than the others. This effect is due to a larger variance in the highly correlated c and d parameters. In the lighter two pion masses, the correlation between these parameters appears to be stronger, leading to a smaller statistical error in the resulting PDFs [64].

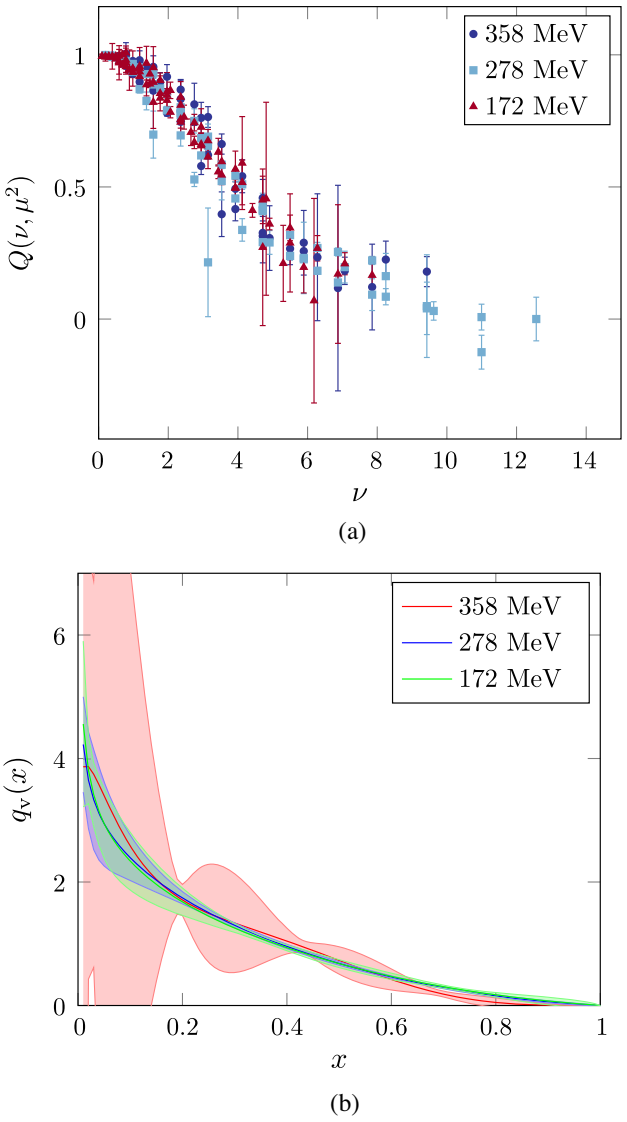

FIG. 3. (a) The $\overline{\text{MS}}$ ITD matched to 2 GeV from the reduced pseudo-ITD results calculated at 358, 278, and 172. (b) The nucleon valence distribution obtained from fitting the ITD to the form in Eq. (13) from each of those ensembles.

Extrapolation to the physical pion mass.—In order to determine the valence PDF for the physical pion mass, our results must be extrapolated to 135 MeV. To do this, the central values of these curves are extrapolated and the errors are propagated. We have performed the extrapolation including and excluding the statistically noisy result from the heaviest pion ensemble. When using all three ensembles, we extrapolate the results using the form

$$q_v(x, \mu^2, m_\pi) = q_v(x, \mu^2, m_0) + a\Delta m_\pi + b\Delta m_\pi^2, \quad (14)$$

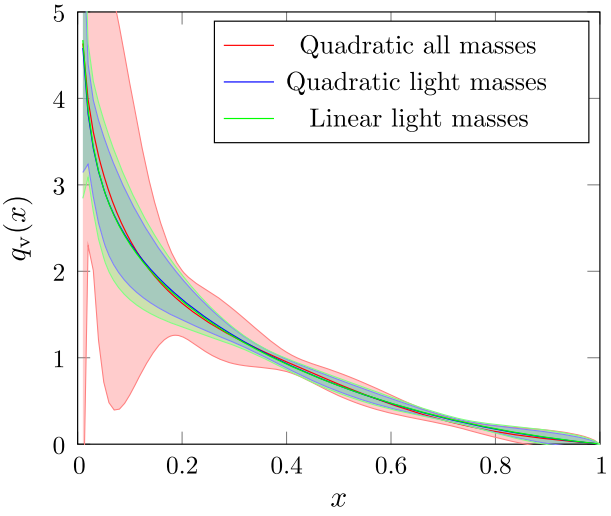

(a)

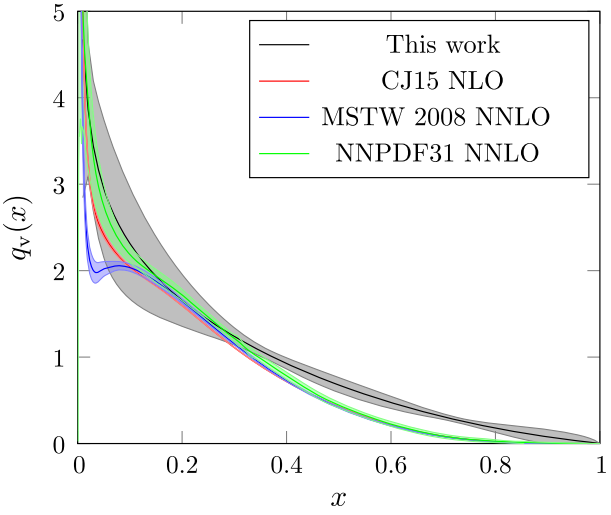

(b)

FIG. 4. (a) The extrapolations of the nucleon valence PDF to physical pion mass. (b) The nucleon valence distribution compared to phenomenological determinations from the NLO global fit CJ15nlo [57] (green), and the NNLO global fits MSTW2008nnlo68cl_nf4 [58] (red) and NNPDF31_nnlo_pch_as_0118_mc_164 [59] (blue) at a reference scale of 2 GeV. A comparison with other lattice determinations at the physical point can be found in [64].

where $\Delta m_\pi = m_\pi - m_0$ and m_0 is the physical pion mass. When using only the two lighter pion mass ensembles, we fix either a or b at zero. Although these extrapolations are not guaranteed to satisfy the normalization of the PDF, we have found them to be close within statistical precision. The extrapolated PDFs are shown in Fig. 4(a). The linear extrapolation with the lightest two ensembles is compared to phenomenological determinations in Fig. 4(b). In both figures, the error bands represent only the statistical error.

The PDF obtained from this fit for $x \gtrsim 0.2$ is larger than the phenomenological fits. This feature is consistent with the larger value of the second moment compared to the global fits in Fig. 2. Other remaining systematic errors could explain this discrepancy. In this Letter, no attempt was made to remove higher-twist effects. Though the estimation of low moments, which relies on low ν, shows no significant sign of higher-twist effects, they could still be present at larger ν, where the ITD becomes more sensitive to higher moments. Also, this calculation was performed on ensembles with a fairly coarse lattice spacing and uses data with $ap \sim O(1)$. Discretization errors have been shown [46] to be potentially significant. Future calculations at smaller lattice spacings are required to control these effects. There are also potentially notable finite volume corrections which may need to be controlled.

Conclusions.—We presented the first calculation of the nucleon PDF based on the method of Ioffe time pseudodistributions performed at the physical pion mass. This is an important step that had to be taken in order to have a more meaningful comparison with the pertinent phenomenological results. Also, by studying three ensembles with different pion masses, we were able to investigate the dependence of the ITD on the pion mass. We saw that it is relatively mild compared to expectations stemming from the studies of $\langle x \rangle$ [61] and calculations of quasi-PDFs [14].

Compared to similar studies, our analysis capitalizes on three key factors: first, the ratio of matrix elements that yields a clean way to avoid all pitfalls and systematics of fixed gauge nonperturbative renormalization; second, the short-distance factorization, which allows for matching to $\overline{\text{MS}}$ without relying on large momentum data with their large statistical noise and potential discretization errors; and third, the summation method, which allows for better control of the excited-state contamination. Having studied finite volume effects and discretization errors in [46], in our upcoming work we plan to study in a systematic way the continuum extrapolation and finite volume, as well as effects stemming from excited-state contamination and higher-twist contributions.

J. K. thanks R. Sufian for the helpful comments. This work is supported by Jefferson Science Associates, LLC, under U.S. DOE Contract No. DE-AC05-06OR23177 (The U.S. Government retains a non-exclusive, paid-up, irrevocable, world-wide license to publish or reproduce this manuscript for U.S. Government purposes.). K. O. was supported in part by U.S. DOE Grant No. DE-FG02-04ER41302. A. V. R. was supported in part by U.S. DOE Grant No. DE-FG02-97ER41028. J. K. was supported in part by the U.S. Department of Energy under Contract No. DE-FG02-04ER41302, Department of Energy Office of Science Graduate Student Research fellowships, through the U.S. Department of Energy, Office of Science, Office of Workforce Development for Teachers and Scientists, Office of Science Graduate Student Research (SCGSR) program and is supported by U.S. Department of Energy Grant No. DE-SC0011941. The authors gratefully acknowledge

the computing time granted by the John von Neumann Institute for Computing (NIC) and provided on the supercomputer JURECA at Jülich Supercomputing Centre (JSC) [62]. We acknowledge the facilities of the USQCD Collaboration, used for this research in part, which are funded by the Office of Science of the U.S. Department of Energy. This work was performed in part using computing facilities at the College of William & Mary, which were provided by contributions from the National Science Foundation (MRI Grant No. PHY-1626177), and the Commonwealth of Virginia Equipment Trust Fund. The authors acknowledge William & Mary Research Computing for providing computational resources and/or technical support that have contributed to the results reported within this Letter. This work used the Extreme Science and Engineering Discovery Environment (XSEDE), which is supported by National Science Foundation Grant No. ACI-1548562 [63]. In addition, this work used resources at NERSC, a DOE Office of Science User Facility supported by the Office of Science of the U.S. Department of Energy under Contract No. DE-AC02-05CH11231, as well as resources of the Oak Ridge Leadership Computing Facility at the Oak Ridge National Laboratory, which is supported by the Office of Science of the U.S. Department of Energy under Contract No. DE-AC05-00OR22725. The software libraries used on these machines were Chroma [65], QUDA [66,67], QDP-JIT [68] and QPhiX [69] developed with support from the U.S. Department of Energy, Office of Science, Office of Advanced Scientific Computing Research and Office of Nuclear Physics, Scientific Discovery through Advanced Computing (SciDAC) program, and of the U.S. Department of Energy Exascale Computing Project.

[1] J. Gao, L. Harland-Lang, and J. Rojo, Phys. Rep. **742**, 1 (2018).
[2] X. Ji, Phys. Rev. Lett. **110**, 262002 (2013).
[3] H.-W. Lin, J.-W. Chen, S. D. Cohen, and X. Ji, Phys. Rev. D **91**, 054510 (2015).
[4] J.-W. Chen, S. D. Cohen, X. Ji, H.-W. Lin, and J.-H. Zhang, Nucl. Phys. **B911**, 246 (2016).
[5] C. Alexandrou, K. Cichy, V. Drach, E. Garcia-Ramos, K. Hadjiyiannakou, K. Jansen, F. Steffens, and C. Wiese, Phys. Rev. D **92**, 014502 (2015).
[6] C. Alexandrou, K. Cichy, M. Constantinou, K. Hadjiyiannakou, K. Jansen, F. Steffens, and C. Wiese, Phys. Rev. D **96**, 014513 (2017).
[7] C. Monahan and K. Orginos, J. High Energy Phys. 03 (2017) 116.
[8] J.-H. Zhang, J.-W. Chen, X. Ji, L. Jin, and H.-W. Lin, Phys. Rev. D **95**, 094514 (2017).
[9] C. Alexandrou, K. Cichy, M. Constantinou, K. Hadjiyiannakou, K. Jansen, H. Panagopoulos, and F. Steffens, Nucl. Phys. **B923**, 394 (2017).
[10] J. Green, K. Jansen, and F. Steffens, Phys. Rev. Lett. **121**, 022004 (2018).
[11] I. W. Stewart and Y. Zhao, Phys. Rev. D **97**, 054512 (2018).
[12] C. Monahan, Phys. Rev. D **97**, 054507 (2018).
[13] W. Broniowski and E. R. Arriola, Phys. Rev. D **97**, 034031 (2018).
[14] C. Alexandrou, K. Cichy, M. Constantinou, K. Jansen, A. Scapellato, and F. Steffens, Phys. Rev. Lett. **121**, 112001 (2018).
[15] J.-W. Chen, L. Jin, H.-W. Lin, Y.-S. Liu, Y.-B. Yang, J.-H. Zhang, and Y. Zhao, arXiv:1803.04393.
[16] C. Alexandrou, K. Cichy, M. Constantinou, K. Jansen, A. Scapellato, and F. Steffens, Phys. Rev. D **98**, 091503(R) (2018).
[17] H.-W. Lin, J.-W. Chen, X. Ji, L. Jin, R. Li, Y.-S. Liu, Y.-B. Yang, J.-H. Zhang, and Y. Zhao, Phys. Rev. Lett. **121**, 242003 (2018).
[18] Z.-Y. Fan, Y.-B. Yang, A. Anthony, H.-W. Lin, and K.-F. Liu, Phys. Rev. Lett. **121**, 242001 (2018).
[19] Y.-S. Liu, J.-W. Chen, L. Jin, R. Li, H.-W. Lin, Y.-B. Yang, J.-H. Zhang, and Y. Zhao, arXiv:1810.05043.
[20] C. Alexandrou, K. Cichy, M. Constantinou, K. Hadjiyiannakou, K. Jansen, A. Scapellato, and F. Steffens, Phys. Rev. D **99**, 114504 (2019).
[21] T. Izubuchi, L. Jin, C. Kallidonis, N. Karthik, S. Mukherjee, P. Petreczky, C. Shugert, and S. Syritsyn, Phys. Rev. D **100**, 034516 (2019).
[22] J. R. Green, K. Jansen, and F. Steffens, Phys. Rev. D **101**, 074509 (2020).
[23] Y. Chai *et al.*, Phys. Rev. D **102**, 014508 (2020).
[24] H.-W. Lin, J.-W. Chen, Z. Fan, J.-H. Zhang, and R. Zhang, arXiv:2003.14128.
[25] W. Detmold and C. J. D. Lin, Phys. Rev. D **73**, 014501 (2006).
[26] V. Braun and D. Müller, Eur. Phys. J. C **55**, 349 (2008).
[27] A. J. Chambers, R. Horsley, Y. Nakamura, H. Perlt, P. E. L. Rakow, G. Schierholz, A. Schiller, K. Somfleth, R. D. Young, and J. M. Zanotti, Phys. Rev. Lett. **118**, 242001 (2017).
[28] J. Liang, T. Draper, K.-F. Liu, A. Rothkopf, and Y.-B. Yang, Phys. Rev. D **101**, 114503 (2020).
[29] Y.-Q. Ma and J.-W. Qiu, Phys. Rev. Lett. **120**, 022003 (2018).
[30] G. S. Bali *et al.*, Eur. Phys. J. C **78**, 217 (2018).
[31] G. S. Bali, V. M. Braun, B. Gläßle, M. Göckeler, M. Gruber, F. Hutzler, P. Korcyl, A. Schäfer, P. Wein, and J.-H. Zhang, Phys. Rev. D **98**, 094507 (2018).
[32] R. S. Sufian, J. Karpie, C. Egerer, K. Orginos, J.-W. Qiu, and D. G. Richards, Phys. Rev. D **99**, 074507 (2019).
[33] G. S. Bali *et al.* (RQCD Collaboration), Eur. Phys. J. A **55**, 116 (2019).
[34] R. S. Sufian, C. Egerer, J. Karpie, R. G. Edwards, B. Joó, Y.-Q. Ma, K. Orginos, J.-W. Qiu, and D. G. Richards, arXiv:2001.04960 [Phys. Rev. D (to be published)].
[35] H.-W. Lin *et al.*, Prog. Part. Nucl. Phys. **100**, 107 (2018).
[36] K. Cichy and M. Constantinou, Adv. High Energy Phys. **2019**, 3036904 (2019).
[37] C. Monahan, Proc. Sci., LATTICE2018 (**2018**) 018 [arXiv:1811.00678].

[38] J.-W. Qiu, J. Phys. Soc. Jpn. Conf. Proc. **26**, 011010 (2019).
[39] A. V. Radyushkin, Phys. Rev. D **96**, 034025 (2017).
[40] B. L. Ioffe, Phys. Lett. **30B**, 123 (1969).
[41] V. Braun, P. Gornicki, and L. Mankiewicz, Phys. Rev. D **51**, 6036 (1995).
[42] K. Orginos, A. Radyushkin, J. Karpie, and S. Zafeiropoulos, Phys. Rev. D **96**, 094503 (2017).
[43] J. Karpie, K. Orginos, A. Radyushkin, and S. Zafeiropoulos, EPJ Web Conf. **175**, 06032 (2018).
[44] J. Karpie, K. Orginos, and S. Zafeiropoulos, J. High Energy Phys. 11 (2018) 178.
[45] J. Karpie, K. Orginos, A. Rothkopf, and S. Zafeiropoulos, J. High Energy Phys. 04 (2019) 057.
[46] B. Joó, J. Karpie, K. Orginos, A. Radyushkin, D. Richards, and S. Zafeiropoulos, J. High Energy Phys. 12 (2019) 081.
[47] B. Joó, J. Karpie, K. Orginos, A. V. Radyushkin, D. G. Richards, R. S. Sufian, and S. Zafeiropoulos, Phys. Rev. D **100**, 114512 (2019).
[48] A. V. Radyushkin, Int. J. Mod. Phys. A **35**, 2030002 (2020).
[49] A. Radyushkin, Phys. Rev. D **98**, 014019 (2018).
[50] J.-H. Zhang, J.-W. Chen, and C. Monahan, Phys. Rev. D **97**, 074508 (2018).
[51] T. Izubuchi, X. Ji, L. Jin, I. W. Stewart, and Y. Zhao, Phys. Rev. D **98**, 056004 (2018).
[52] G. Altarelli and G. Parisi, Nucl. Phys. **B126**, 298 (1977).
[53] C. R. Allton *et al.* (UKQCD Collaboration), Phys. Rev. D **47**, 5128 (1993).
[54] G. S. Bali, B. Lang, B. U. Musch, and A. Schäfer, Phys. Rev. D **93**, 094515 (2016).
[55] C. Bouchard, C. C. Chang, T. Kurth, K. Orginos, and A. Walker-Loud, Phys. Rev. D **96**, 014504 (2017).
[56] B. Yoon *et al.*, Phys. Rev. D **95**, 074508 (2017).
[57] A. Accardi, L. T. Brady, W. Melnitchouk, J. F. Owens, and N. Sato, Phys. Rev. D **93**, 114017 (2016).
[58] A. D. Martin, W. J. Stirling, R. S. Thorne, and G. Watt, Eur. Phys. J. C **63**, 189 (2009).
[59] R. D. Ball *et al.* (NNPDF Collaboration), Eur. Phys. J. C **77**, 663 (2017).
[60] K. Cichy, L. Del Debbio, and T. Giani, J. High Energy Phys. 10 (2019) 137.
[61] M. Constantinou, Proc. Sci., LATTICE2014 (**2015**) 001 [arXiv:1411.0078].
[62] Jülich Supercomputing Centre, J. Large-Scale Res. Facil. **4**, A132 (2018).
[63] J. Towns, T. Cockerill, M. Dahan, I. Foster, K. Gaither, A. Grimshaw, V. Hazlewood, S. Lathrop, D. Lifka, G. D. Peterson, R. Roskies, J. Scott, and N. Wilkins-Diehr, Comput. Sci. Eng. **16**, 62 (2014).
[64] See Supplemental Material at http://link.aps.org/supplemental/10.1103/PhysRevLett.125.232003 for more details.
[65] R. G. Edwards and B. Joo, Nucl. Phys. B Proc. Suppl. **140**, 832 (2005)..
[66] M. A. Clark, R. Babich, K. Barros, R. C. Brower, and C. Rebbi, Comput. Phys. Commun. **181**, 1517 (2010).
[67] R. Babich, M. A. Clark, and B. Joo, SC 10 (Supercomputing 2010) Report No. JLAB-IT-10-01 (2010).
[68] B. Joó, D. D. Kalamkar, K. Vaidyanathan, M. Smelyanskiy, K. Pamnany, V. W. Lee, P. Dubey, and W. Watson, Lect. Notes Comput. Sci. **7905**, 40 (2013)..
[69] F. T. Winter, M. A. Clark, R. G. Edwards, and B. Joó, *28th IEEE International Parallel and Distributed Processing Symposium* (IEEE, 2014).